J. Biochem. **138**, 763–772 (2005)
doi:10.1093/jb/mvi168

Hematopoietic Tissue–Specific Expression of Mouse *Neil3* for Endonuclease VIII–Like Protein

Kumiko Torisu, Daisuke Tsuchimoto*, Yoshinori Ohnishi and Yusaku Nakabeppu
Division of Neurofunctional Genomics, Department of Immunobiology and Neuroscience, Medical Institute of Bioregulation, Kyushu University, 3-1-1 Maidashi Higashi-ku, Fukuoka 812-8582

Received June 9, 2005; accepted September 12, 2005

We cloned cDNA and genomic DNA containing exon 1 of mouse *Neil3*. *Neil3* spans 52.4 kb and consists of 10 exons. Northern blot analysis revealed that *Neil3* mRNA was selectively expressed in thymus, spleen and bone marrow. High levels of *Neil3* mRNA were also detected in various mouse B cell lines by RT-PCR. Immunofluorescence microscopy using anti-NEIL3 revealed that recombinant mouse NEIL3 is localized in the nuclei. In mouse splenocytes, the level of *Neil3* mRNA significantly increased after mitogen stimulation in vitro. We established NEIL3-null mice, which are viable and fertile. We found candidate sequences for NEIL3 orthologues in a DNA database from dog and zebrafish in addition to human and mouse, but not invertebrates. NEIL3 may function exclusively in vertebrates, such as mammals.

Key words: base excision repair, DNA glycosylase, gene targeting, *Neil3*.

Abbreviations: APEX2, apurinic/apyrimidinic endonuclease 2; ConA, concanavalin A; ES cell, embryonic stem cell; LPS, lipopolysaccharide; MutM, formamidopyrimidine DNA glycosylase; Nei, endonuclease VIII; NEIL3, nei-like 3; Nth, endonuclease III; 8-oxoG, 8-oxoguanine; Tg, thymine glycol.

Reactive oxygen species are generated during normal cellular metabolism or exposure to environmental agents. DNA is attacked by reactive oxygen species and its oxidation causes various alterations in the chemistry of bases, sugars and phosphates. Such DNA damage may result in mutagenesis or cell death, ultimately causing various age-related diseases such as cancer and neurodegeneration (*1*, *2*). Among the various oxidized bases, 8-oxoguanine (8-oxoG) and thymine glycol (Tg) have been well characterized because of their abundance and biological significance. The formation of an 8-oxoG:A mismatch has been demonstrated to be one of the major spontaneous causes for a G:C to T:A transversion mutation (*3*), while Tg blocks DNA replication and thus causes cell death (*4*). These damaged bases are known to be excised by DNA glycosylase and repaired through the base excision repair system. In *Escherichia coli*, formamidopyrimidine DNA glycosylase (MutM) for excision of 8-oxoG opposite cytosine in DNA, and endonuclease III (Nth) or endonuclease VIII (Nei) for excision of oxidized pyrimidine lesions including Tg in duplex DNA, respectively, are DNA glycosylases which suppress both mutagenesis and cell death caused by reactive oxygen species (*5*, *6*).

In mammals, 8-oxoguanine DNA glycosylase (OGG1) is a functional homologue of MutM, and endonuclease III–like 1 (NTHL1/NTH1) is an Nth orthologue; and both fulfill a similar function to their counterparts in *E. coli* (*7–12*). In addition, three human proteins which are homologous to Nei have recently been identified and designated Nei-like (NEIL) 1, NEIL2 and NEIL3 (*13–16*). NEIL1 and NEIL2 possess DNA glycosylase and AP lyase activities and engage in excising various oxidized bases (*13*, *14*, *16–20*). Recently, it has been reported that NEIL1 and 2 show a unique preference for excising 5-hydroxyuracil or 8-oxoG from a DNA bubble (*21*). As for the function of NEIL3, Morland *et al*. (*15*) reported increased excision of methyl-formamidopyrimidines (methyl-FapyG) from duplex DNA by extracts of recombinant human NEIL3–expressing insect cells, but there has been no report of a study using a purified preparation of NEIL3.

We have identified and characterized a second mammalian AP endonuclease, APEX2, from both human and mouse (*22–24*). In the present study, we found that human and mouse NEIL3 proteins possess a C-terminal region similar to that of APEX2. We therefore isolated mouse cDNA and found that the mouse *Neil3* gene was preferentially expressed in thymus, spleen and bone marrow. We then isolated the mouse *Neil3* gene and established NEIL3-null mice. Furthermore, we found that expression of *Neil3* mRNA in splenocytes was induced by mitogen stimulation.

MATERIALS AND METHODS

Synthetic Oligonucleotides—Synthetic oligonucleotides used as PCR primers were purchased from the Hokkaido System Science Co. Ltd. (Sapporo, Japan) and Fasmac (Tokyo, Japan): NEIL3-ORF1, 5′-ACAGCCATGGTGGAAGGACCAGG-3′; NEIL3-ORF2, 5′-TGTGATGCTTGCTTGACCTCAAGG-3′; NEIL3-ORF3, 5′-CCAAATGCAGTTTTCCTGTTG-3′; NEIL3-ORF4, 5′-AAGAGGATCCTATTAGCATCCTGG-3′, NEIL3-E5, 5′-GCTGCTCCAATGAATGC-3′; NEIL3-E6, 5′-TGCCTCCCCTTGTTTTC-3′.

Sequence Analysis—DNA or amino acid sequence database searches were carried out with NCBI BLAST (http://www.ncbi.nlm.nih.gov/BLAST/). Information regarding

*To whom correspondence should be addressed. Tel: +81-92-642-6802, Fax: +81-92-64-6804, E-mail: daisuke@bioreg.kyushu-u.ac.jp

the region 5′ upstream and the neighboring genes of mouse *Neil3* (ENSMUSG00000039396) and human *NEIL3* (ENSG00000109674) was obtained from the Trust Sanger Institute (http://www.sanger.ac.uk/). The transcription start point and cis-element motif sequences were predicted with the NIX application at the UK HGMP Resource Center (http://menu.hgmp.mrc.ac.uk/menu-bin/Nix/) and MOTIF (Sequence Motif Search, http://www.motif.genome.jp/)

Isolation of Mouse Neil3 cDNA and Genomic Clones—*Neil3* cDNA was amplified by PCR from a mouse spleen cDNA library prepared from a C57BL/6 mouse, a gift from Dr. J. O-Wang (Kyushu University, Japan), using the primers NEIL3-ORF1, NEIL3-ORF2, NEIL3-ORF3, and NEIL3-ORF4. Amplified fragments were subcloned into pT7Blue T vector (Novagen, Madison, MA) to generate the plasmids pT7Blue:Neil3-5′half and pT7Blue:Neil3–3′half, and were combined at the *Stu*I site to generate pT7Blue:Neil3ORF, which includes the entire *Neil3* ORF. Two partially overlapping phage genomic clones carrying *Neil3* exon 1 (λNeil3-1 and λNeil3-2) were isolated from a λTK genomic library (a gift from Dr. D. E. Rancourt, University of Calgary, Canada) constructed in a λ TK phage with 129/SvJ mouse genomic DNA using a fragment containing the *Neil3* exon 1 sequence as a probe, by means of retro-recombination screening (*25*).

Cell Culture—NIH3T3 and HEK293T cells were grown in MEM with 10% calf serum and DMEM with 10% fetal bovine serum, respectively, and each medium was supplemented with 100 U/ml penicillin and 100 μg/ml streptomycin. A20 cells were obtained from American Type Culture Collection (ATCC, Manassas, VA) and maintained in the medium which they recommended. Primary mouse splenocytes were cultured as described by Ide *et al*. (*24*). When required, cells were stimulated with 20 μg/ml lipopolysaccharide (LPS) or 4 μg/ml concanavalin A (ConA). CCE embryonic stem (ES) cells derived from a 129/Sv/Ev mouse were cultured as previously described (*26*).

Northern Blot Analysis—Total RNA samples from mouse tissues were obtained from Clontech (Palo Alto, CA) except heart and lung, which were purchased from Stratagene (La Jolla, CA). Total RNA samples prepared from human tissues were purchased from Clontech. Northern blot analysis was performed as previously described (*27*). Human *NEIL3* and mouse *Neil3* total cDNA amplified by PCR from a human *NEIL3* cDNA clone (Accession No. NM018248, provided by Helix Research Institute, Chiba, Japan) and a mouse spleen cDNA library, respectively, were used as probes.

RT-PCR—Total cellular RNA was prepared using an Isogen kit (Nippon Gene, Tokyo, Japan) according to the manufacturer's instructions. First-strand cDNAs were prepared using First-Strand cDNA Synthesis kits (Amersham Biosciences, Little Chalfont, UK). To amplify *Neil3* cDNA, templates were subjected to 30 cycles of PCR (98°C for 1 s, 50°C for 5 s, and 72°C for 15 s) with the primers NEIL3-E5 and NEIL3-E6. RT-PCR for *Gapdh* mRNA was performed as previously described (*28*). For each sample, PCR was also performed for fewer and more than 30 cycles, and we regarded the results of PCR with 30 cycles as semiquantitative when the amounts of PCR products were proportional to PCR cycle numbers in this range.

Plasmid Constructions—A plasmid pET32a (+):NEIL3 (1–282) encoding TrxA-NEIL3(1–282) was prepared by inserting a *Neil3* cDNA fragment encoding the 282 N-terminal amino acids into *Nco*I–*Bam*HI sites of pET32a (+) (Novagen) using PCR. Plasmids pIRES2-EGFP:NEIL3 and pcDNA3.1:NEIL3 were constructed by introducing a *Bam*HI–*Bam*HI fragment prepared from pT7Blue: Neil3ORF was introduced into the *Bam*HI site of pIRES2- EGFP (Clontech) and pcDNA3.1/hyg. (Clontech), respectively.

Anti–Mouse NEIL3 Antibody—Rabbit polyclonal antibodies against fusion protein TrxA-NEIL3(1–282) were prepared as previously described (*29*). The antibodies were purified using antigen affinity columns prepared with TrxA-NEIL3(1–282)-Sepharose and TrxA-Sepharose columns (*22*). The purified antibodies were designated anti-NEIL3.

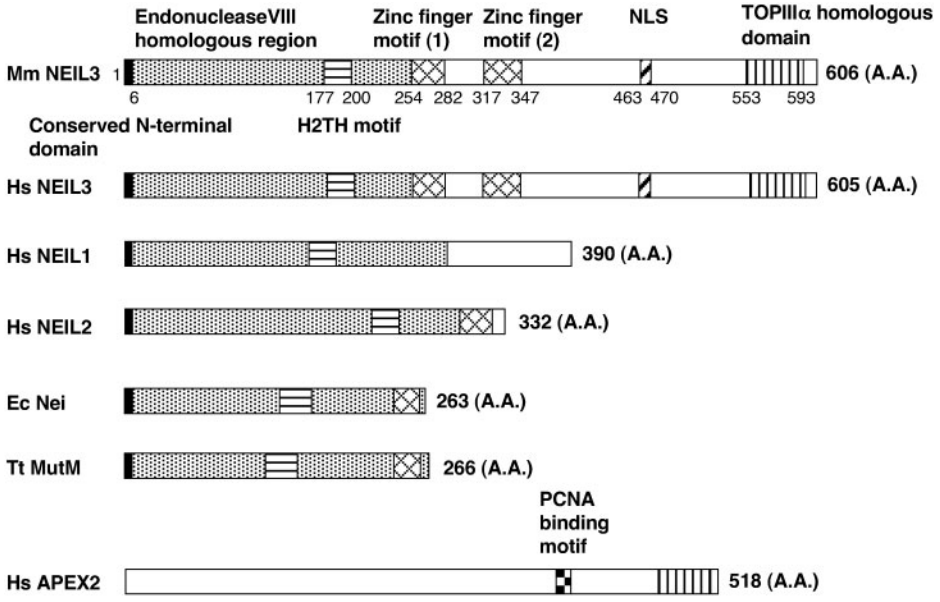

Fig. 1. **Structures of mouse/human NEIL3 proteins and other homologous proteins.** Structures of mouse/human NEIL3, human NEIL1, NEIL2, *E. coli* Nei, *Thermus thermophilus* MutM and human APEX2 are shown. The region conserved in the MutM/Nei family (1–282 aa of Mm NEIL3) and the unique C-terminal region of NEIL3 (283–606 aa of Mm NEIL3) are indicated. Black boxes, the conserved N-terminal domain; horizontally-striped box, H2TH motif; cross-hatched box, zinc finger motifs; hatched box, putative nuclear localization signals; vertically-striped box, topoisomerase IIIα homologous domain; checkered box, PCNA binding motif.

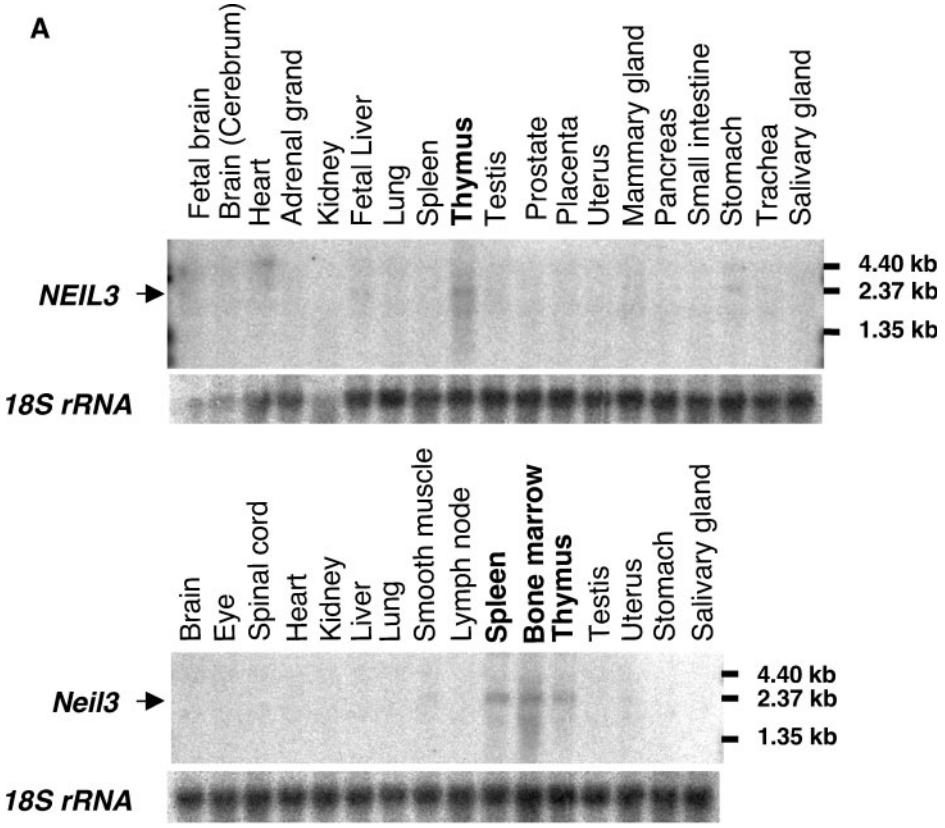

Fig. 2. **Expression of *Neil3/NEIL3* mRNA in human and mouse tissues.** (A) Northern blot analysis of *Neil3*/*NEIL3* in human and mouse tissues. Total RNA (20 μg) prepared from various human and mouse tissues was electrophoresed, transferred onto membranes and hybridized with ^{32}P-labeled probes for human *NEIL3*, mouse *Neil3* and 18S rRNAs. The arrow indicates *Neil3*/*NEIL3* mRNA. (B) Semiquantitative RT-PCR for *Neil3* mRNA in various mouse cell lines. Amplification of *Neil3* and *Gapdh* cDNA is shown in the upper panel and the lower panel, respectively, and the relative amount of *Neil3* mRNA to *Gapdh* mRNA is shown under each lane. From the left, BW5147.3, T cell; BAF, pro B cell; 70Z/3, pre B cell; WEHI-231, immature B cell; A20, mature B cell; p3u1, myeloma cell; WEHI-3 and J774A.1, macrophage; NIH3T3 and BALB/c3T3, fibroblast.

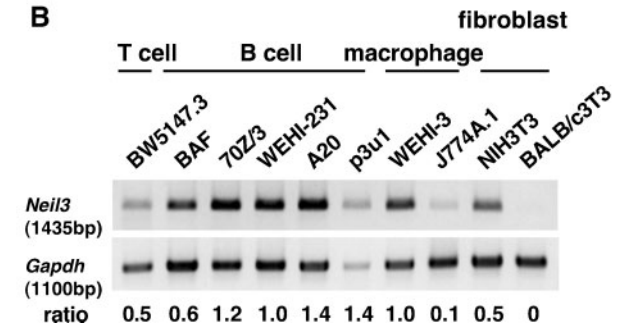

Western Blotting—Western blot analyses were performed as previously described (*22*), using anti-NEIL3 (2.0 μg/ml), anti-MLH1 (4.0 μg/ml) (*30*) and anti-HSP60 (2.0 μg/ml) (Stressgen Bioreagents Co., BC, Canada).

Immunofluorescence Microscopy—HEK293T cells were plated in a collagen I–coated 6-well plate (BD Biosciences, Bedford, MA) and transfected with pIRES2-EGFP:NEIL3 and pIRES2-EGFP using Effectene Transfection Reagent (QIAGEN, Hilden, Germany). After 24 h of incubation, the cells were reseeded onto a collagen I–coated 2-well chamber slide (BD Biosciences) and cultured for 24 h. The cells were fixed with 4% paraformaldehyde and permeabilized in 0.3% Tween 20 and 0.1% Triton X-100. Nonspecific binding was blocked with 1% BSA solution. Next, the cells were stained with 2.0 μg/ml anti-NEIL3 followed by 6.7 μg/ml Alexa Fluor 594–conjugated goat anti-rabbit (Molecular Probes, OR). For nuclear staining, the slides were incubated with 50 ng/ml DAPI (Sigma, St. Louis, MO) for 20 min. The slides were observed under an AxioPhoto microscope (Carl Zeiss, Oberkochen, Germany) equipped with an AxioCam microscopic digital camera (Carl Zeiss). Digital images were processed for publication using Axiovision 3.1 (Carl Zeiss) and Adobe Photoshop 5.5 J (Adobe Systems).

Southern Blotting—Genomic DNAs extracted from ES cells were digested with *Xba*I or *Hin*dIII. Southern hybridization was performed as previously described (*23*).

Immunoprecipitation—All procedures were performed at 4°C. The thymocytes and splenocytes derived from wild-type and homozygous mutant mice were suspended in 1 ml of lysis buffer [50 mM Tris-HCl pH 7.5, 500 mM NaCl, 1.0% NP-40, 1% Protease Inhibitor Cocktail (Nacalai Tesque Inc., Kyoto Japan)], and disrupted by sonication. Cell lysates were centrifuged, and 0.5 ml of the supernatant was incubated with protein A–Sepharose (Amersham Biosciences) and 20 μg of normal rabbit IgG. After centrifugation, supernatant was incubated with 3 μg of anti-NEIL3 for 1 h, then protein A–Sepharose was added and the mixture was incubated for 1 h. After centrifugation, the precipitated products were subjected to Western blot analysis.

Subcellular Fractionation—All procedures were performed at 4°C. Nuclear and cytoplasmic fractions were prepared as described previously (*31*). Briefly, thymocytes were suspended in hypotonic NP-40 buffer [10 mM Tris-HCl pH 7.5, 10 mM NaCl, 0.5% NP-40, 1% Protease Inhibitor Cocktail (Nacalai Tesque Inc)] and incubated for 10 min. After centrifugation at 300 × *g* for 5 min, precipitated nuclei were re-suspended in 1 ml of the lysis buffer.

NaCl, Tris-HCl and NP-40 were added to the supernatant to adjust their concentrations to those of the lysis buffer. The nuclei suspension and the adjusted supernatant were sonicated and centrifuged at 100,000 × *g* for 30 m. Supernatants of both samples were collected as nuclear and cytoplasmic fractions respectively, and subjected to immunoprecipitation with anti-NEIL3 in the same way as the whole-cell extract described above. Aliquots of each fraction were analyzed by Western blot analysis using anti-HSP60 (mitochondrial marker) or anti-MLH1 (nuclear marker) to confirm the quality of the fractionation.

Targeted Disruption of the Neil3 Gene—A targeting vector of *Neil3* was constructed as follows. A region of genomic DNA containing *Neil3* exon 1 in λNeil3-2 DNA, which was excised by *Bam*HI digestion (Fig. 4B), was replaced with a *Sal*I fragment containing a pol II-*neo*-poly(A) cassette (*32*). To join the non-cohesive ends, each was converted to a 2-base cohesive end by partial filling in with Klenow fragment in the presence of dATP and dGTP for the *Bam*HI site or dCTP and dGTP for the *Sal*I site. Then 50 μg of *Sal*I fragment excised from the targeting vector was introduced into CCE ES cells (5×10^7 cells) by electroporation as previously described (*26*, *33*). The colonies were expanded in the presence of 250 μg/ml G418 (Sigma) and 5 μM Ganciclovir (Nippon Syntex, Tokyo, Japan) and were then selected.

Establishment of Neil3 Chimera and Heterozygous Mutant Mice—Heterozygous mutant ES cells were injected into blastocysts from C57BL/6 J mice (CLEA Japan, Tokyo Japan). The resultant male chimeras obtained were mated with female C57BL/6 J mice.

RESULTS

NEIL3 Protein Shares Sequence Homology with E. coli Endonuclease VIII and MutM—We searched for proteins with a sequence similar to the C-terminal region (314–518 amino acids) of human APEX2, and retrieved human NEIL3 (DDBJ/EMBL/GenBank Accession No. NP060718). The amino acid sequence of human NEIL3 was used to search the mouse expressed sequence tag (EST) database for cDNA of the mouse orthologue. Two potential EST clones (Accession Nos. BG917244 and AA254703) were identified. The obtained sequences were used to design new primers and the entire *Neil3* cDNA was amplified by PCR using the above primers from a mouse spleen cDNA library. The sequence of mouse *Neil3* cDNA was deposited in the DDBJ Data Library (Accession No. AB072931).

The mouse *Neil3* gene is located on Chromosome 8B3.1, and is flanked by the *Aspartylglucosaminidase* (*Aga*) gene 63 kb from its 3′ end, and by *Vascular endothelial growth factor c* (*Vegfc*) gene more than 400 kb from its 5′ end. Mouse NEIL3 protein consists of 606 amino acids, with a predicted molecular weight of 67 kDa. NEIL3 protein exhibits partial homology to the MutM/Nei family of proteins as summarized in Fig. 1. The N-terminal domain necessary for the catalytic activity of DNA glycosylase/AP lyase, the DNA-binding-helix-two-turns-helix (H2TH) motif and the zinc finger DNA-binding motif conserved in MutM/Nei family proteins were all found in the N-terminal half of NEIL3. In the conserved N-terminal domain consisting of six amino acid residues (PEL/GPEV), valine replaces the Pro2 residue in mouse and human NEIL3.

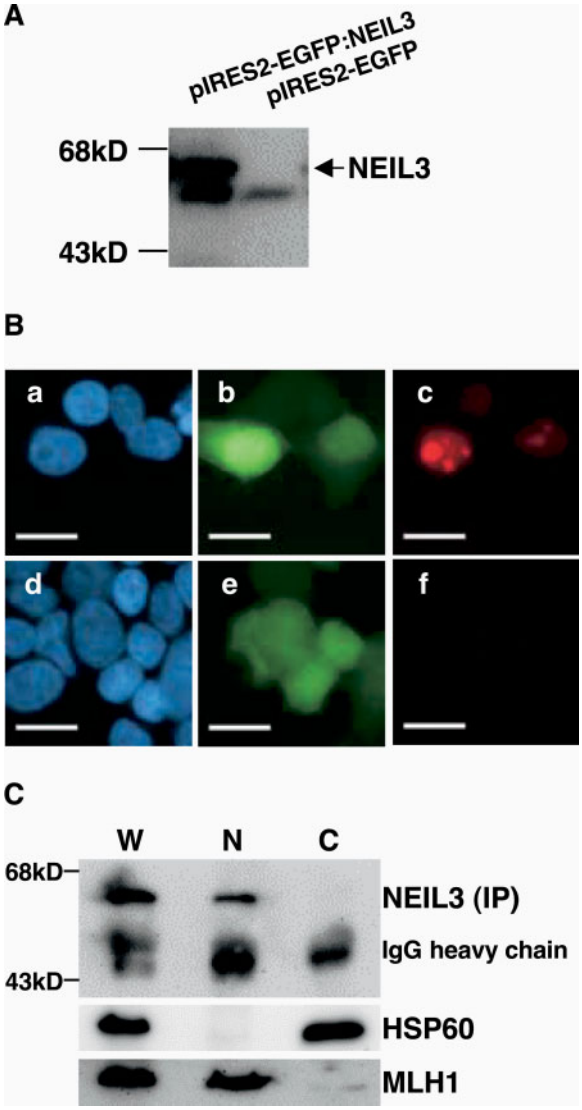

Fig. 3. **Subcellular localization of mouse NEIL3.** (A) Western blot analysis of recombinant mouse NEIL3 protein. HEK293T cells were transiently transfected with pIRES2-EGFP and pIRES2-EGFP:NEIL3. Recombinant NEIL3 in whole-cell lysates (20 μg protein per lane) of HEK293T cells was detected by Western blotting using anti-NEIL3. The arrow indicates the recombinant mouse NEIL3. (B) Distribution of NEIL3 protein in the nuclei. HEK293T cells were transfected transiently with pIRES2-EGFP:NEIL3 (a, b, c) and pIRES2-EGFP (d, e, f). The cells were examined with an immunofluorescence microscope, using anti-NEIL3 in combination with Alexa Fluor 594–labeled second antibody. Nuclei were counterstained with DAPI. [EGFP: (b, e), green, NEIL3: (c, f), red, DNA: (a, d), blue] Bars: 50 μm (C) Subcellular localization of endogenous NEIL3. Whole-cell (W), nuclear (N) and cytoplasmic (C) extracts were prepared from thymocytes of C57BL/6 J male mice. NEIL3 protein was then precipitated with anti-NEIL3 and analyzed by Western blotting using anti-NEIL3. Samples derived from 5×10^7 cells were loaded into each lane. The quality of each fractionated extract from 10^6 cells was monitored by Western blotting using anti-HSP60 (mitochondrial marker) or anti-MLH1 (nuclear marker).

NEIL3 possesses a C-terminal extension (324 aa) in addition to the N-terminal half, and the C-terminal region contains the second zinc finger DNA-binding motif, nuclear localization signal and a subregion similar to the

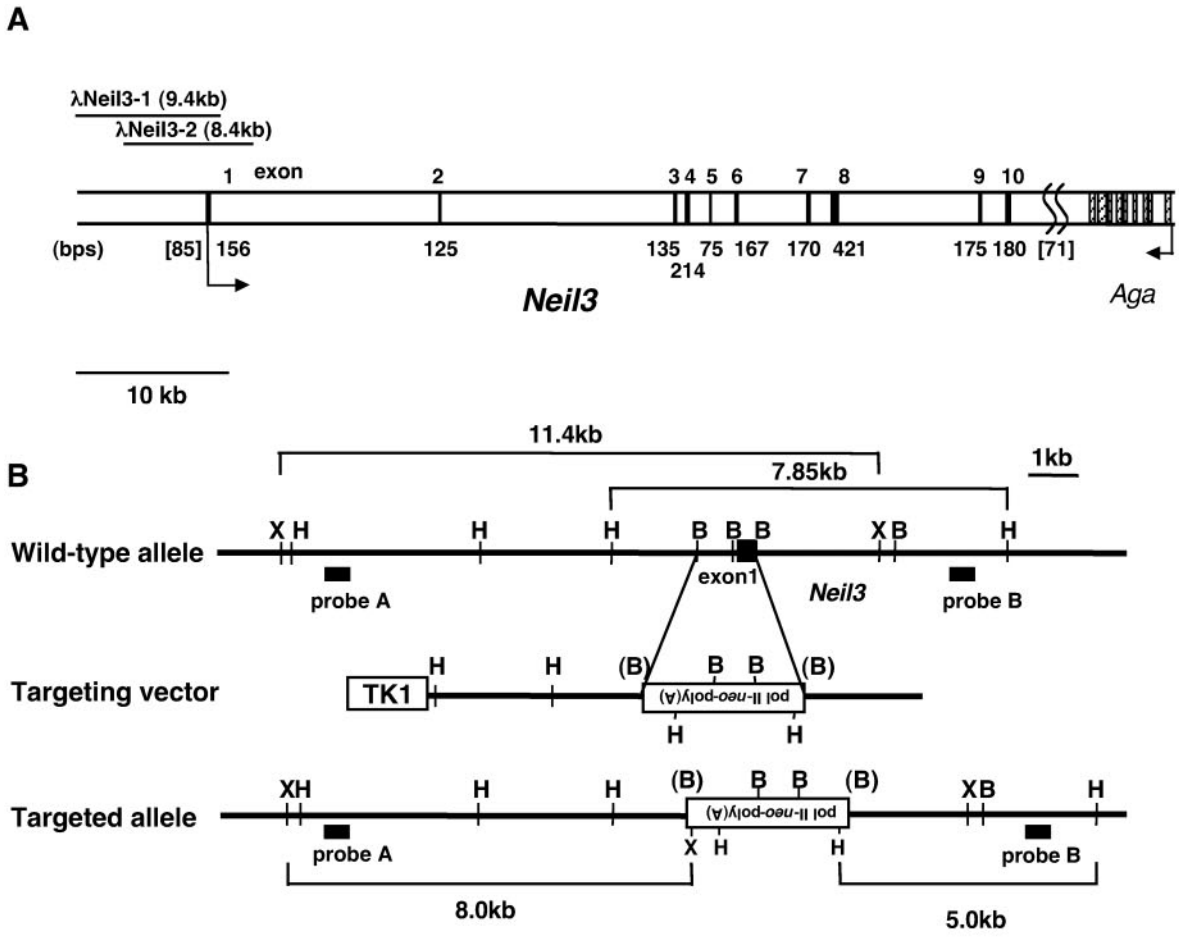

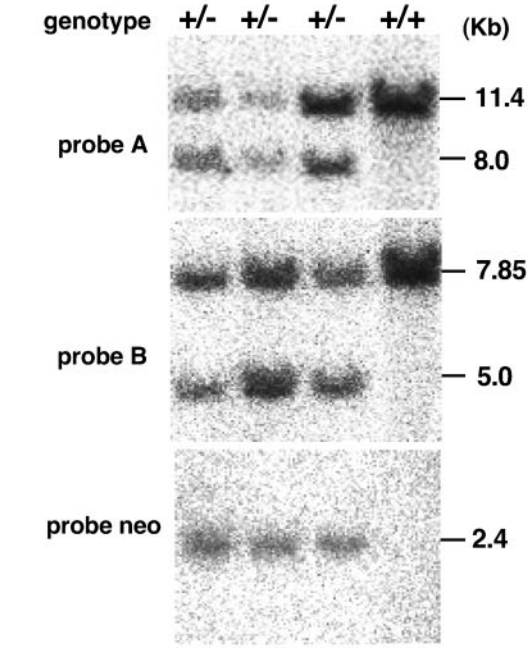

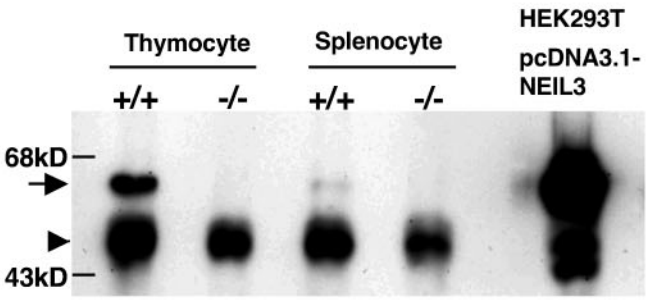

C-terminal regions of human DNA topoisomerase IIIα or APEX2. This subregion contains tandem repeated zinc ribbon domains, which are present in *E. coli* topoisomerase I, human transcription elongation factor SII (TfIIS) (*34*), RNA polymerase transcription termination factor (TTF2) (*15*), as well as in topoisomerase IIIα and APEX2. APEX2, but not NEIL3, possesses a typical PCNA-binding motif (Qxxhxxaa) in the C-terminal region.

Neil3 Is Preferentially Expressed in Hematopoietic Tissues—Tissue expression patterns of mouse *Neil3* and human *NEIL3* were compared by Northern blot analyses (Fig. 2A). A single major band corresponding to approximately 2.3-kb mRNA was detected in both mouse and human tissues. Mouse *Neil3* mRNA was detected only in thymus, spleen and bone marrow, while human *NEIL3* mRNA was detected only in thymus. In other mouse and human tissues, the transcript was barely detectable, suggesting that *Neil3* or *NEIL3* preferentially expresses in hematopoietic tissues.

To examine expression of the mouse *Neil3* gene in various cells of hematopoietic lineage, semiquantitative RT-PCRs for *Neil3* mRNA were performed using RNA prepared from mouse cell lines (Fig. 2B). A relatively high level of *Neil3* mRNA was detected in NIH3T3 but not in BALB/c 3T3 fibroblast cells. Most of the mouse hematopoietic cell lines examined expressed higher levels of *Neil3* mRNA than the fibroblast cell lines. Among the former, B-cell lines expressed the highest levels of *Neil3* mRNA. There was no apparent relationship between the level of *Neil3* mRNA and the stage of B-cell maturation.

Subcellular Localization of Mouse NEIL3 Protein—Anti-NEIL3 was prepared and purified as described in Materials and Methods. The anti-NEIL3 specifically detected a 60 kDa recombinant mouse NEIL3 expressed in HEK293T cells by Western blot analysis (Fig. 3A). Next, immunofluorescence microscopy with anti-NEIL3 was performed on HEK293T cells transfected with a plasmid, pIRES2-EGFP or pIRES2-EGFP:NEIL3. As shown in Fig. 3B, only EGFP-positive cells exhibited apparent nuclear foci of NEIL3 when pIRES2-EGFP:NEIL3, but not pIRES2-EGFP, was introduced, indicating that most of the native form of mouse NEIL3 was localized in the nucleus. The nuclear foci of NEIL3 were mostly located in regions with a lower DAPI fluorescence, suggesting that the foci were located in euchromatin regions. Essentially the same results were obtained with mouse embryonic fibroblasts (data not shown). Finally, we analyzed the subcellular localization of endogenous NEIL3 protein in mouse thymocytes. Nuclear and cytoplasmic fractions were prepared from thymocytes of 5-week-old C57BL/6 J male mice, and both fractions were subjected to immunoprecipitation with anti-NEIL3. Western blot analysis of precipitated samples revealed that endogeneous NEIL3 is located exclusively in nuclei.

Generation of NEIL3-Null Mice—To explore the *in vivo* function of NEIL3, we carried out targeted disruption of the *Neil3* gene in mouse ES cells. The mouse genomic database revealed that the *Neil3* gene spans 52.4 kb and consists of 10 exons (Fig. 4A). A region containing the entire sequence of exon 1 (725 bp) was replaced by a *neo* cassette in opposite orientation in order to construct the targeted allele *Neil3*^{tm1Yun} (Fig. 4B). Exon 1 contains the initiation codon and encodes the N-terminal catalytic residues (Fig. 1). ES clones in which one of the *Neil3*$^{+}$ alleles was replaced with the *Neil3*^{tm1Yun} allele by homologous recombination were confirmed by Southern blot analysis (Fig. 4C).

Heterozygous mutant mice (*Neil3*$^{+/tm1Yun}$) were established as described in Materials and Methods, and homozygous mutant mice (*Neil3*$^{tm1Yun/tm1Yun}$, *Neil3* KO mice) were obtained by a cross between heterozygous mice. Genotypes were analyzed by PCR with the use of tail DNA (data not shown). Among 299 live-born mice obtained by the cross, 64 *Neil3* KO mice were identified as being consistent with Mendelian segregation (Table 1). To confirm disruption of the functional *Neil3* gene, we examined the expression of NEIL3 protein in thymocytes and splenocytes prepared from *Neil3* KO mice (Fig. 4D). A band corresponding to the endogenous NEIL3 (60 kDa) detected in thymocytes and splenocytes from wild-type mice completely disappeared in samples from *Neil3* KO mice, demonstrating that *Neil3* KO mice are NEIL3-null.

NEIL3-null mice are viable and apparently healthy for at least 24 weeks after birth. These wild-type and NEIL3-null mice are now under long-term observation. Both male and female NEIL3-null mice proved to be fertile, and homozygous offspring obtained by crossing these mice were also found to be healthy (data not shown).

Regulation of Neil3 Gene Expression—The expression level of endogenous NEIL3 protein in young mice is higher in thymocytes than in splenocytes, as shown in Fig. 4D. In these young animals, a large portion of thymocytes actively

Fig. 4. **Genomic structure and targeted disruption of *Neil3*.** (A) Genomic structure of the *Neil3* gene. The structure of the gene, with the restriction enzyme sites (X, *Xba*I; H, *Hin*dIII; B, *Bam*HI), is shown. Exons are boxed in black, and the number and length of each are shown above and under the exon (the length of untranslated regions is shown in parentheses), respectively. Shaded boxes represent the exons for *Aspartylgulcosaminidase*. Alignment of DNA fragments derived from the mouse genomic library is shown in the upper part. The approximate insert size of each clone is shown in parentheses. (B) Targeting of *Neil3* by homologous recombination. The wild-type *Neil3* allele, a targeting vector and the mutant *Neil3* allele (*Neil3*^{tm1Yun}) are shown at the top, middle and bottom, respectively. White boxes represent a positive [pol II-*neo*-poly(A)] or a negative (HSV-*tk*) selection cassette; the thick lines indicate genomic sequences of the region around *Neil3* exon 1. Lettered bars show 5′ external hybridization probe A and 3′ external hybridization probe B. The expected sizes of the diagnostic restriction fragments used to distinguish the wild-type and mutant alleles are shown in thin lines. (C) Southern blot analysis of *Neil3*. Genomic DNA was prepared from wild-type (+/+) and heterozygous mutant (+/–) ES cells. *Xba*I-digested genomic DNA was probed with the external 5′ probe A, which detects an 11.4-kb wild-type fragment and an 8.0-kb mutated fragment (upper panel). *Hin*dIII-digested genomic DNA was probed with the external 3′ probe B, which detects a 7.85-kb wild-type fragment and a 5.0-kb mutated fragment (middle panel). A 2.4-kb fragment from mutant-type was detected with a probe for pol II-*neo*-poly(A) (lower panel). (D) NEIL3 protein was not detected in NEIL3-null mice. Thymocytes and splenocytes (2.5×10^8 cells each) isolated from wild-type (+/+) and *Neil3* KO (–/–) mice (4-weeks-old), were subjected to immunoprecipitation using anti-NEIL3, and the precipitated products were analyzed by Western blotting using the same antibody. The precipitated products derived from 1×10^8 cells were added to each lane and separated by SDS-PAGE. The recombinant mouse NEIL3 expressed transiently in HEK293T cells was loaded as a positive control. The arrow shows an endogenous NEIL3 and recombinant NEIL3, and the arrowhead indicates IgG heavy chain.

Table 1. **Genotypes of progeny from intermatings of heterozygous mice (*Neil3*$^{+/tm1Yun}$, F1).**

Sex	Genotype, no.		
	WT	Heterozygous	KO
Male	35	81	32
Female	38	81	32
Total (ratio)	73 (1)	162 (2.2)	64 (0.9)

Heterozygous, *Neil3*$^{+/tm1Yun}$; KO, *Neil3*$^{tm1Yun/tm1Yun}$.

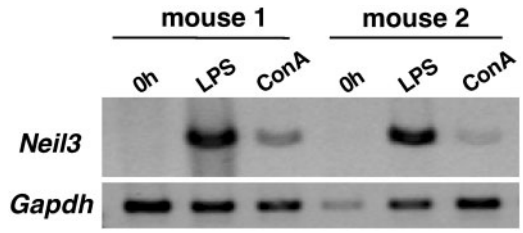

Fig. 5. **Induction of *Neil3* mRNA expression in mouse splenocytes after mitogen stimulation.** The splenocytes (2×10^7 cells) prepared from C57BL/6 J mice (8 weeks old), were cultured for 48 h in medium including LPS (20 μg/ml) or ConA (4 μg/ml). Using total RNA derived from uncultured and cultured splenocytes, RT-PCR for *Neil3* and *Gapdh* mRNA was performed. Two independent results from different mice (1 and 2) are shown.

proliferate, while splenocytes are mostly in the quiescent (G_0) state. To examine whether the expression of *Neil3* is dependent on the proliferation status, the expression level of *Neil3* mRNA in splenocytes with or without mitogen stimulation was determined by semiquantitative RT-PCR (Fig. 5). Splenocytes prepared from C57BL/6 J mice were incubated with LPS or ConA. *Neil3* mRNA in the splenocytes before mitogen stimulation (0 h) was barely detectable under these experimental conditions. However, a marked increase in *Neil3* mRNA was observed 48 h after LPS stimulation. ConA also increased the *Neil3* mRNA level but to a much lesser degree than with LPS stimulation.

DISCUSSION

In the present study, we cloned and characterized the mouse *Neil3* gene and its cDNA, and furthermore analyzed its gene expression and promoter function. There have been a few reports characterizing the human *NEIL3* gene structure (*14*) and functions of recombinant human NEIL3 protein (*15*, *16*). In mouse, the cloning of *Neil3* cDNA was previously reported (*17*), but no further studies have emerged.

Human and mouse NEIL3 proteins are identical in 74% of amino acid residues. The N-terminal half of NEIL3 shares partial homology with members of the MutM/Nei family, and conserved residues in this family corresponding to Lys53, His68, Asn169 and Arg253 in *E. coli* Nei (*20*) are also conserved in NEIL3. The N-terminal proline in NEIL3 is replaced with valine. One group has previously reported that recombinant NEIL3 may excise methyl-FapyG from duplex DNA using crude extracts (*15*).

Many repair proteins involved in the BER pathway, including APEX2 (*23*) and uracil-DNA glycosylase (UNG) (*35*), are expressed in thymus as well as in other organs, but, the preferred expression in hematopoietic tissues is quite unique to the *Neil3*/*NEIL3* gene (Fig. 2). Putative proteins homologous to NEIL3 have been reported in dog and zebrafish (Accession Nos. XM532851 and NM001007335) but not in invertebrates. Invertebrates do not contain antigen-specific lymphocytes, while even the earliest jawed vertebrates harbor antibody molecules (*36*). This suggests that NEIL3 might have appeared in vertebrates during evolution and function in lymphocytes. In addition, we must stress that NEIL3 may play roles in other immune cells, such as macrophages, dendritic cells and granulocytes, since these cells are also present in spleen and can be activated by mitogen stimulation.

As shown in Fig. 6A, we predicted that in mouse, the position 86 bases upstream from the translation initiation codon may serve as the transcription initiation site (+1) based on analysis using the NIX application at the UK HGMP Resource Center. At around the +1 position, we found a sequence in which six out of seven nucleotides are identical to the initiator (Inr) consensus sequence (PyPyANT/APyPy) and which followed the GC-rich Sp1-binding sequence but not the TATA box in the region up to -1000. We further found a downstream promoter element (DPE) 32 bases downstream of the Inr. The transcription initiation site of human *NEIL3* has already been determined and appears in the genomic database of the Trust Sanger Institute as located within a candidate sequence for the Inr. The 5′ end of the longest strand of mouse *Neil3* cDNA (Accession No. BY324102) from the full-length cDNA project starts within this region (*37*), whereas the longest human *NEIL3* cDNA (Accession No. BP380910) begins 36 bases upstream from the estimated +1 position, indicating that there may be multiple transcription initiation sites in human *NEIL3*.

As shown in Fig. 6B, we found various putative *cis*-acting elements involved in lymphocyte-specific gene expression within the entire promoter region. Ikaros, GATA-3, RUNX1, c-Ets-1, NF-AT and NF-κB are all transcriptional factors required for aspects of normal lymphoid development including maturation and mitogenic activation (*36*, *38*).

NEIL3-null mice look healthy for at least 24 weeks after birth. Northern blot analysis has revealed *NEIL3* expression in human testis (*15*), but we did not detect *Neil3* expression in mouse testis. Furthermore, NEIL3-null male mice were able to reproduce, indicating that NEIL3 is not required for maintenance of testis function. With a mixed genetic background of 129/Sv/Ev and C57BL/6 J, NEIL3-null mice exhibited a tendency of reduction of peripheral white blood cell number (data not shown). In our study, NEIL3-null mice were maintained in specific-pathogen-free rooms, so that the exposure of these mice to strong foreign antigens or pathogenic microbes would likely be necessary to induce an obvious phenotype because of the preferred expression of *Neil3* gene in lymphoid organs. Aging may also increase DNA damage and induce abnormalities in NEIL3-null lymphocytes. To analyze hematopoiesis and immunological response in NEIL3-null mice with a homogeneous genetic background, we are now repeating intercrosses of *Neil3*$^{+/tm1\ Yun}$ mice with C57BL/6 J.

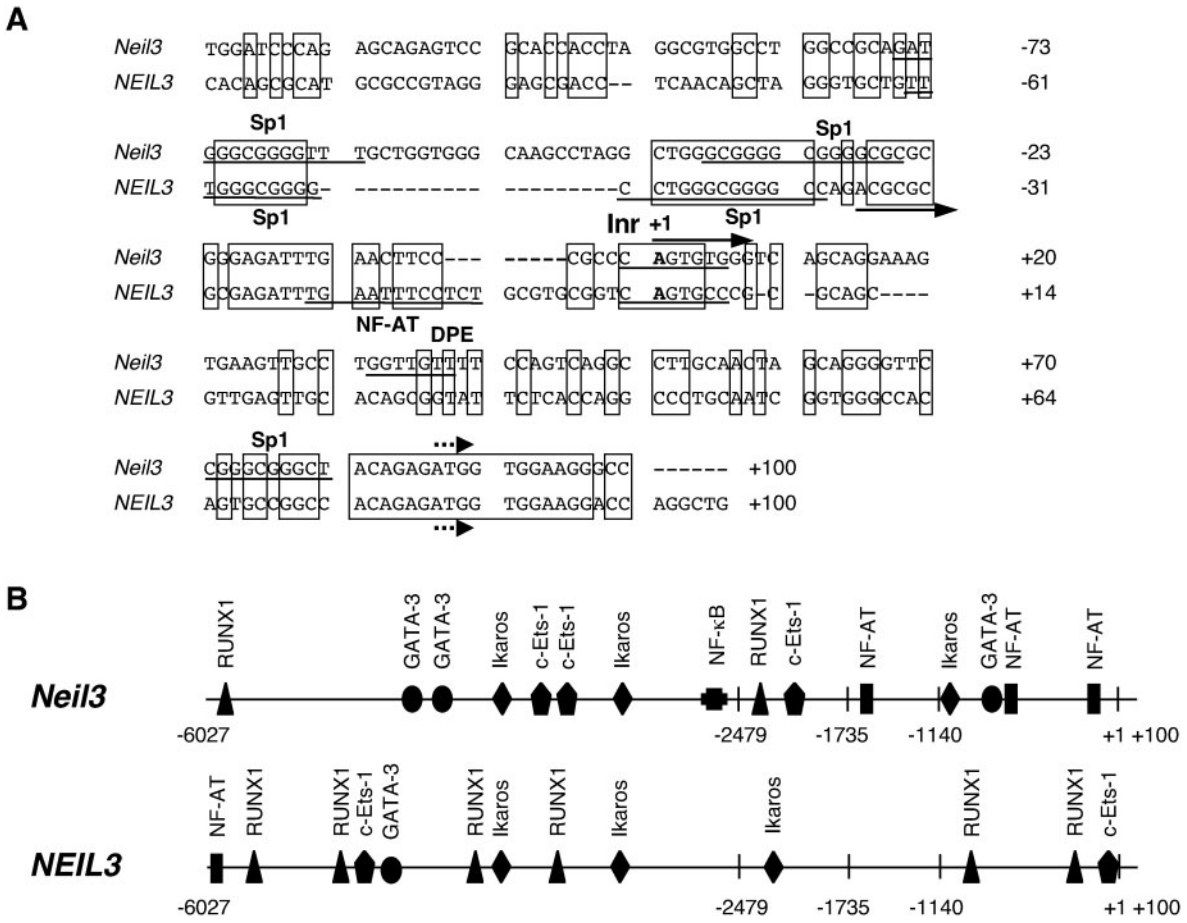

Fig. 6. **Analysis of the 5′ upstream region of mouse *Neil3* and human *NEIL3*.** (A) Alignment of the genomic sequences of the *Neil3* and *NEIL3* genes with their 5′ upstream regions. Identical residues are boxed. Numbering in bp is indicated to the right. The transcription initiation sites (+1) of *Neil3* and *NEIL3*, indicated in bold, were determined as described in the "DISCUSSION." The translation initiation codons are indicated with dotted arrows. The potential Inr and DPE consensus sequences and putative binding sequences for Sp1 and NF-AT are underlined. The black arrows indicate the longest strand of *Neil3* cDNA and *NEIL3* cDNA (Accession Nos. BY324102 and BP380910) above and below their sequences, respectively. (B) The putative *cis*-acting elements that are involved in lymphocyte-specific gene expression within the region from –6027 to +100 of the *Neil3* and *NEIL3* genes. These elements exhibit more than 90% similarity to each consensus sequence in MOTIF.

We thank Daniel Nathans for NIH3T3 and BALB/c3T3 cells, Motoya Katsuki for CCE ES cells, Manabu Nakashima for HEK293T and mouse hematopoietic cell lines, and Derrick E. Rancourt for the λ TK library. We also wish to thank Mizuki Ohno, Kunihiko Sakumi and Knut Woltjen for their helpful discussions, Masumi Ohtsu, Yukari Yamada, Akemi Matsuyama and Keiko Aiura for their technical assistance, and William Campbell for comments on the manuscript. This work was supported by grants from the CREST Japan Science and Technology Agency, the Ministry of Education, Culture, Sports, Science, and Technology of Japan (16012248), and the Japan Society for the Promotion of Science (15590347 and 16390119).

REFERENCES

1. Friedberg, E.C., Walker, G.C., and Siede, W. (1995) *DNA Repair and Mutagenesis*, American Society of Microbiology, Washington, DC, WA
2. Nakabeppu, Y., Tsuchimoto, D., Furuichi, M., and Sakumi, K. (2004) The defense mechanisms in mammalian cells against oxidative damage in nucleic acids and their involvement in the suppression of mutagenesis and cell death. *Free Radic. Res.* **38**, 423–429
3. Shibutani, S., Takeshita, M., and Grollman, A.P. (1991) Insertion of specific bases during DNA synthesis past the oxidation-damaged base 8-oxodG. *Nature* **349**, 431–434
4. Laspia, M.F. and Wallace, S.S. (1988) Excision repair of thymine glycols, urea residues, and apurinic sites in *Escherichia coli*. *J. Bacteriol.* **170**, 3359–3366
5. Michaels, M.L., Pham, L., Cruz, C., and Miller, J.H. (1991) MutM, a protein that prevents G.C—T.A transversions, is formamidopyrimidine-DNA glycosylase. *Nucleic Acids Res.* **19**, 3629–3632
6. Jiang, D., Hatahet, Z., Blaisdell, J.O., Melamede, R.J., and Wallace, S.S. (1997) *Escherichia coli* endonuclease VIII: cloning, sequencing, and overexpression of the *nei* structural gene and characterization of *nei* and *nei nth* mutants. *J. Bacteriol.* **179**, 3773–3782
7. Radicella, J.P., Dherin, C., Desmaze, C., Fox, M.S., and Boiteux, S. (1997) Cloning and characterization of *hOGG1*, a human homolog of the *OGG1* gene of *Saccharomyces cerevisiae*. *Proc. Natl. Acad. Sci. USA* **94**, 8010–8015
8. Arai, K., Morishita, K., Shinmura, K., Kohno, T., Kim, S.R., Nohmi, T., Taniwaki, M., Ohwada, S., and Yokota, J. (1997) Cloning of a human homolog of the yeast *OGG1* gene that is

involved in the repair of oxidative DNA damage. *Oncogene* **14**, 2857–2861
9. Aburatani, H., Hippo, Y., Ishida, T., Takashima, R., Matsuba, C., Kodama, T., Takao, M., Yasui, A., Yamamoto, K., and Asano, M. (1997) Cloning and characterization of mammalian 8-hydroxyguanine-specific DNA glycosylase/apurinic, apyrimidinic lyase, a functional mutM homologue. *Cancer Res.* **57**, 2151–2156
10. Aspinwall, R., Rothwell, D.G., Roldan-Arjona, T., Anselmino, C., Ward, C.J., Cheadle, J.P., Sampson, J.R., Lindahl, T., Harris, P.C., and Hickson, I.D. (1997) Cloning and characterization of a functional human homolog of *Escherichia coli* endonuclease III. *Proc. Natl Acad. Sci. USA* **94**, 109–114
11. Ikeda, S., Biswas, T., Roy, R., Izumi, T., Boldogh, I., Kurosky, A., Sarker, A.H., Seki, S., and Mitra, S. (1998) Purification and characterization of human NTH1, a homolog of *Escherichia coli* endonuclease III. Direct identification of Lys-212 as the active nucleophilic residue. *J. Biol. Chem.* **273**, 21585–21593
12. Sarker, A.H., Ikeda, S., Nakano, H., Terato, H., Ide, H., Imai, K., Akiyama, K., Tsutsui, K., Bo, Z., Kubo, K., Yamamoto, K., Yasui, A., Yoshida, M.C., and Seki, S. (1998) Cloning and characterization of a mouse homologue (mNthl1) of *Escherichia coli* endonuclease III. *J. Mol. Biol.* **282**, 761–774
13. Hazra, T.K., Izumi, T., Boldogh, I., Imhoff, B., Kow, Y.W., Jaruga, P., Dizdaroglu, M., and Mitra, S. (2002) Identification and characterization of a human DNA glycosylase for repair of modified bases in oxidatively damaged DNA. *Proc. Natl Acad. Sci. USA* **99**, 3523–3528
14. Bandaru, V., Sunkara, S., Wallace, S.S., and Bond, J.P. (2002) A novel human DNA glycosylase that removes oxidative DNA damage and is homologous to *Escherichia coli* endonuclease VIII. *DNA Repair* **1**, 517–529
15. Morland, I., Rolseth, V., Luna, L., Rognes, T., Bjoras, M., and Seeberg, E. (2002) Human DNA glycosylases of the bacterial Fpg/MutM superfamily: an alternative pathway for the repair of 8-oxoguanine and other oxidation products in DNA. *Nucleic Acids Res.* **30**, 4926–4936
16. Takao, M., Kanno, S., Kobayashi, K., Zhang, Q.M., Yonei, S., van der Horst, G.T., and Yasui, A. (2002) A back-up glycosylase in *Nth1* knock-out mice is a functional Nei (endonuclease VIII) homologue. *J. Biol. Chem.* **277**, 42205–42213
17. Rosenquist, T.A., Zaika, E., Fernandes, A.S., Zharkov, D.O., Miller, H., and Grollman, A.P. (2003) The novel DNA glycosylase, NEIL1, protects mammalian cells from radiation-mediated cell death. *DNA Repair* **2**, 581–591
18. Katafuchi, A., Nakano, T., Masaoka, A., Terato, H., Iwai, S., Hanaoka, F., and Ide, H. (2004) Differential specificity of human and *Escherichia coli* endonuclease III and VIII homologues for oxidative base lesions. *J. Biol. Chem.* **279**, 14464–14471
19. Hazra, T.K., Kow, Y.W., Hatahet, Z., Imhoff, B., Boldogh, I., Mokkapati, S.K., Mitra, S., and Izumi, T. (2002) Identification and characterization of a novel human DNA glycosylase for repair of cytosine-derived lesions. *J. Biol. Chem.* **277**, 30417–30420
20. Wallace, S.S., Bandaru, V., Kathe, S.D., and Bond, J.P. (2003) The enigma of endonuclease VIII. *DNA Repair* **2**, 441–453
21. Dou, H., Mitra, S., and Hazra, T.K. (2003) Repair of oxidized bases in DNA bubble structures by human DNA glycosylases NEIL1 and NEIL2. *J. Biol. Chem.* **278**, 49679–49684
22. Tsuchimoto, D., Sakai, Y., Sakumi, K., Nishioka, K., Sasaki, M., Fujiwara, T., and Nakabeppu, Y. (2001) Human APE2 protein is mostly localized in the nuclei and to some extent in the mitochondria, while nuclear APE2 is partly associated with proliferating cell nuclear antigen. *Nucleic Acids Res.* **29**, 2349–2360
23. Ide, Y., Tsuchimoto, D., Tominaga, Y., Iwamoto, Y., and Nakabeppu, Y. (2003) Characterization of the genomic structure and expression of the mouse *Apex2* gene. *Genomics* **81**, 47–57
24. Ide, Y., Tsuchimoto, D., Tominaga, Y., Nakashima, M., Watanabe, T., Sakumi, K., Ohno, M., and Nakabeppu, Y. (2004) Growth retardation and dyslymphopoiesis accompanied by G_2/M arrest in APEX2-null mice. *Blood* **104**, 4097–4103
25. Woltjen, K., Bain, G., and Rancourt, D.E. (2000) Retrorecombination screening of a mouse embryonic stem cell genomic library. *Nucleic Acids Res.* **28**, E41
26. Robertson, E.J. (1987) *Teratocarcinomas and Embryonic Stem Cells: A Practical Approach*, IRL Press, New York, NY
27. Oda, S., Nishida, J., Nakabeppu, Y., and Sekiguchi, M. (1995) Stabilization of cyclin E and cdk2 mRNAs at G_1/S transition in Rat-1A cells emerging from the G_0 state. *Oncogene* **10**, 1343–1351
28. Ichinoe, A., Behmanesh, M., Tominaga, Y., Ushijima, Y., Hirano, S., Sakai, Y., Tsuchimoto, D., Sakumi, K., Wake, N., and Nakabeppu, Y. (2004) Identification and characterization of two forms of mouse MUTYH proteins encoded by alternatively spliced transcripts. *Nucleic Acids Res.* **32**, 477–487
29. Nakabeppu, Y. and Nathans, D. (1991) A naturally occurring truncated form of FosB that inhibits Fos/Jun transcriptional activity. *Cell* **64**, 751–759
30. Kawate, H., Itoh, R., Sakumi, K., Nakabeppu, Y., Tsuzuki, T., Ide, F., Ishikawa, T., Noda, T., Nawata, H., and Sekiguchi, M. (2000) A defect in a single allele of the *Mlh1* gene causes dissociation of the killing and tumorigenic actions of an alkylating carcinogen in methyltransferase-deficient mice. *Carcinogenesis* **21**, 301–305
31. Nakabeppu, Y., Oda, S., and Sekiguchi, M. (1993) Proliferative activation of quiescent Rat-1A cells by ΔFosB. *Mol Cell Biol* **13**, 4157–4166
32. Deng, C., Thomas, K.R., and Capecchi, M.R. (1993) Location of crossovers during gene targeting with insertion and replacement vectors. *Mol. Cell Biol.* **13**, 2134–2140
33. Joyner, A.L. (1993) *Gene Targeting: A Practical Approach*, IRL Press, New York
34. Krishna, S.S., Majumdar, I., and Grishin, N.V. (2003) Structural classification of zinc fingers: survey and summary. *Nucleic Acids Res.* **31**, 532–550
35. Haug, T., Skorpen, F., Aas, P.A., Malm, V., Skjelbred, C., and Krokan, H.E. (1998) Regulation of expression of nuclear and mitochondrial forms of human uracil-DNA glycosylase. *Nucleic Acids Res.* **26**, 1449–1457
36. Abbas, A.K., Lichitman, A.H., and Pober, J.S. (2000) *Cellular and Molecular Immunology*, W.B. Saunders company, Philadelphia, PA
37. Okazaki, Y., Furuno, M., Kasukawa, T., Adachi, J., Bono, H., Kondo, S., Nikaido, I., Osato, N., Saito, R., Suzuki, H., Yamanaka, I., Kiyosawa, H., Yagi, K., Tomaru, Y., Hasegawa, Y., Nogami, A., Schonbach, C., Gojobori, T., Baldarelli, R., Hill, D.P., Bult, C., Hume, D.A., Quackenbush, J., Schriml, L.M., Kanapin, A., Matsuda, H., Batalov, S., Beisel, K.W., Blake, J.A., Bradt, D., Brusic, V., Chothia, C., Corbani, L.E., Cousins, S., Dalla, E., Dragani, T.A., Fletcher, C.F., Forrest, A., Frazer, K.S., Gaasterland, T., Gariboldi, M., Gissi, C., Godzik, A., Gough, J., Grimmond, S., Gustincich, S., Hirokawa, N., Jackson, I.J., Jarvis, E.D., Kanai, A., Kawaji, H., Kawasawa, Y., Kedzierski, R.M., King, B.L., Konagaya, A., Kurochkin, I.V., Lee, Y., Lenhard, B., Lyons, P.A., Maglott, D.R., Maltais, L., Marchionni, L., McKenzie, L., Miki, H., Nagashima, T., Numata, K., Okido, T., Pavan, W.J., Pertea, G., Pesole, G., Petrovsky, N., Pillai, R., Pontius, J.U., Qi, D., Ramachandran, S., Ravasi, T., Reed, J.C., Reed, D.J., Reid, J., Ring, B.Z., Ringwald, M., Sandelin, A., Schneider, C., Semple, C.A., Setou, M., Shimada, K., Sultana, R., Takenaka, Y., Taylor, M.S., Teasdale, R.D., Tomita, M., Verardo, R., Wagner, L., Wahlestedt, C., Wang, Y., Watanabe, Y., Wells, C., Wilming, L.G., Wynshaw-Boris, A., Yanagisawa, M., Yang, I., Yang, L., Yuan, Z., Zavolan, M., Zhu, Y., Zimmer, A., Carninci, P.,

Hayatsu, N., Hirozane-Kishikawa, T., Konno, H., Nakamura, M., Sakazume, N., Sato, K., Shiraki, T., Waki, K., Kawai, J., Aizawa, K., Arakawa, T., Fukuda, S., Hara, A., Hashizume, W., Imotani, K., Ishii, Y., Itoh, M., Kagawa, I., Miyazaki, A., Sakai, K., Sasaki, D., Shibata, K., Shinagawa, A., Yasunishi, A., Yoshino, M., Waterston, R., Lander, E.S., Rogers, J., Birney, E., and Hayashizaki, Y. (2002) Analysis of the mouse transcriptome based on functional annotation of 60,770 full-length cDNAs. *Nature* **420**, 563–573

38. Shivdasani, R.A. and Orkin, S.H. (1996) The transcriptional control of hematopoiesis. *Blood* **87**, 4025–4039